Reduction of *S*-nitrosoglutathione by alcohol dehydrogenase 3 is facilitated by substrate alcohols via direct cofactor recycling and leads to GSH-controlled formation of glutathione transferase inhibitors

Claudia A. STAAB*†, Johan ÅLANDER†, Margareta BRANDT*, Johan LENGQVIST*[1], Ralf MORGENSTERN†, Roland C. GRAFSTRÖM† and Jan-Olov HÖÖG*[2]

*Department of Medical Biochemistry and Biophysics, Karolinska Institutet, SE-171 77 Stockholm, Sweden, and †Institute of Environmental Medicine, Karolinska Institutet, SE-171 77 Stockholm, Sweden

GSNO (*S*-nitrosoglutathione) is emerging as a key regulator in NO signalling as it is in equilibrium with S-nitrosated proteins. Accordingly, it is of great interest to investigate GSNO metabolism in terms of competitive pathways and redox state. The present study explored ADH3 (alcohol dehydrogenase 3) in its dual function as GSNOR (GSNO reductase) and glutathione-dependent formaldehyde dehydrogenase. The glutathione adduct of formaldehyde, HMGSH (*S*-hydroxymethylglutathione), was oxidized with a k_{cat}/K_m value approx. 10 times the k_{cat}/K_m value of GSNO reduction, as determined by fluorescence spectroscopy. HMGSH oxidation *in vitro* was greatly accelerated in the presence of GSNO, which was concurrently reduced under cofactor recycling. Hence, considering the high cytosolic NAD^+/NADH ratio, formaldehyde probably triggers ADH3-mediated GSNO reduction by enzyme-bound cofactor recycling and might result in a decrease in cellular S-NO (S-nitrosothiol) content *in vivo*. Formaldehyde exposure affected S-NO content in cultured cells with a trend towards decreased levels at concentrations of 1–5 mM, in agreement with the proposed mechanism. Product formation after GSNO reduction to the intermediate semimercaptal responded to GSH/GSNO ratios; ratios up to 2-fold allowed the spontaneous rearrangement to glutathione sulfinamide, whereas 5-fold excess of GSH favoured the interception of the intermediate to form glutathione disulfide. The sulfinamide and its hydrolysis product, glutathione sulfinic acid, inhibited GST (glutathione transferase) activity. Taken together, the findings of the present study provide indirect evidence for formaldehyde as a physiological trigger of GSNO depletion and show that GSNO reduction can result in the formation of GST inhibitors, which, however, is prevented under normal cellular redox conditions.

Key words: cofactor recycling, metabolic interaction, protein S-nitrosation, redox state, S-nitrosothiol, xenobiotic metabolism.

INTRODUCTION

ADH3 (alcohol dehydrogenase 3) [1], also referred to as GSNOR [GSNO (*S*-nitrosoglutathione) reductase] or glutathione-dependent formaldehyde dehydrogenase, is a conserved and ubiquitous enzyme with a broad range of substrate alcohols. Most efficiently, ADH3 catalyses the oxidation of formaldehyde in the form of HMGSH (*S*-hydroxymethylglutathione) and the reduction of GSNO under concomitant conversion of NAD(H) [2–4]. As a consequence of the latter reaction, ADH3 perturbs the cellular equilibrium between GSNO and protein S-NOs (S-nitrosothiols). Thus ADH3 indirectly governs the incidence of protein S-nitrosation (also referred to as S-nitrosylation), which underlies a large part of cellular NO signalling, essential for a wide spectrum of cellular functions and pathways [5,6]. The importance of GSNO in these processes is reflected by the common association of disturbed GSNO levels with disease [7–9]. It has been suggested that GSNO in airway lining fluid protects from asthma; depletion of GSNO by ADH3 correlated with decreased levels of S-nitrosated proteins in adjacent lung epithelial cells and was associated with airway hyper-responsivity [10,11]. In addition, a recent report provides evidence for the association between genetic variation in ADH3 and childhood asthma risk [12].

The cellular ratio of free NAD^+/NADH is typically high [13,14] and is thus considered unfavourable for reductive pathways such as GSNO reduction, but favourable for oxidation under concomitant reduction of NAD^+, e.g. ADH-mediated alcohol oxidation. ADH3 catalyses the oxidation of formaldehyde by converting its glutathione adduct HMGSH and thereby constitutes the primary defence mechanism against formaldehyde damage [3]. Formaldehyde is mainly considered an inhalation toxicant [15], but is also liberated during the metabolism of endogenous compounds as well as xenobiotics [16–18]. Demonstrating considerable effects at low concentrations, formaldehyde exacerbates asthma symptoms although only comparatively small amounts reach the lung [19]. The molecular mechanisms behind this phenomenon are poorly understood. Thus it is of importance to understand how ADH3-mediated GSNO reduction is influenced by formaldehyde (in the form of HMGSH) in particular, but also ADH3 substrates in general.

Conflicting findings have been reported for product formation after NADH-dependent GSNO reduction to the intermediate semimercaptal *S*-(*N*-hydroxyamino)glutathione by ADH3 [4,20,21]. Previous studies have suggested glutathione sulfinamide [4,20] or GSSG [20,21] as major products, the latter requiring GSH for product formation. The physiological significance of

Abbreviations used: ADH3, alcohol dehydrogenase 3; a.m.u., atomic mass unit; CDNB, 1-chloro-2,4-dinitrobenzene; DTPA, diethylenetriaminepentaacetic acid; DTT, dithiothreitol; EMHA, epithelial medium with high levels of amino acids; ESI, electrospray ionization; GSNO, *S*-nitrosoglutathione; GSNOR, GSNO reductase; GST, glutathione transferase; HMGSH, *S*-hydroxymethylglutathione; MGST1, microsomal GST1; S-NO, S-nitrosothiol.

[1] Present address: Karolinska Biomics Center, Karolinska University Hospital, Solna, SE-171 76 Stockholm, Sweden.
[2] To whom correspondence should be addressed (email jan-olov.hoog@ki.se).

© The Authors Journal compilation © 2008 Biochemical Society

the sulfinamide is still unclear and no studies have so far addressed whether it is metabolized further. *In vitro*, glutathione sulfinamide is in part spontaneously hydrolysed to the corresponding sulfinic acid [4,20]. A similar compound, glutathionesulfonic acid, is known to be an inhibitor for GSTs (glutathione transferases) [22,23], enzymes responsible for the GSH-dependent biotransformation of carcinogenic, mutagenic, toxic and pharmacologically active compounds including those formed during oxidative stress.

The present study assessed whether ADH3-mediated GSNO reduction is triggered or inhibited by formaldehyde in the initial absence of NADH, thus mimicking a high cellular NAD^+/NADH ratio. In efforts to determine the physiological products of the reaction, we examined how different ratios of GSH/GSNO affect product yield, using purified ADH3 as well as crude liver cell lysates. Finally, GSNO and the ADH3-mediated products glutathione sulfinamide and sulfinic acid were tested as inhibitors of MGST1 (microsomal GST1).

EXPERIMENTAL

Enzyme purification and chemicals

Recombinant human ADH3 was expressed in *Escherichia coli* and purified to homogeneity in a three-step procedure [24]. After ion-exchange chromatography, the pooled fractions were dialysed and applied to a 5-ml Blue-Sepharose 6 Fast Flow column (GE Healthcare) and eluted with 200 mM NaCl and 5 mM NAD^+. A final gel-filtration step (HiLoad 16/60, Superdex 200; GE Healthcare) was performed in 10 mM Tris/HCl (pH 8.0), 200 mM NaCl and 1 mM DTT (dithiothreitol). The purity of the protein was verified by SDS/PAGE. The protein concentration was measured by amino acid analysis using a Biochrom 20 Plus ninhydrin-based analyser (GE Healthcare) to determine the molar absorption coefficient (ε) at 280 nm (37 900 $M^{-1} \cdot cm^{-1}$), used in all further determinations. Rat MGST1 was purified as described previously [25].

All chemicals were purchased from Sigma–Aldrich unless otherwise stated. Formaldehyde solutions were made from newly opened glass ampoules [20 % solutions (Ladd Research Industries, Williston, VT, U.S.A.) or 16 % solutions (Polysciences, Eppelheim, Germany)]. Ethanol (Kemetyl) and octanol (Merck) were of analytical grade. GSNO was prepared as described by Hart [26]; it was of comparable quality to purchased GSNO (Sigma–Aldrich) as assessed by absorption spectroscopy (peaks at 336 and 545 nm) and initial rate studies of ADH3-mediated GSNO reduction. Upon synthesis, GSNO was stored at −20 °C in the dark. GSNO, GSH and NADH solutions were always protected from light and kept on ice.

Enzyme kinetics

Steady-state kinetics for the ADH3 substrates HMGSH and GSNO including the inhibition constant for GSH were performed in 0.1 M potassium phosphate (pH 7.5) containing 2.4 mM NAD^+ and 1 mM GSH for HMGSH oxidation, and 0.1 mM NADH and different GSH concentrations for GSNO reduction respectively. GSNO concentrations were varied from 5 to 60 μM. Enzyme concentrations in the assays were 0.25 μg/ml (6.25 nM per monomer). GSH solutions were prepared in 0.1 M potassium phosphate buffer (pH 7.5). All solutions were de-aerated for studies of GSNO reduction. Enzymatic activity was monitored by following the increase in fluorescence at 455 nm ($\lambda_{ex} = 340$ nm) in a fluorescence microplate reader (Tecan Infinite M200) at 25 °C. HMGSH concentrations were calculated as previously described with a K_{eq} of 1.77 for adduct dissociation [27] and they ranged from 0.07 to 1.44 μM. Initial rates for NADH production/consumption were determined by using standard curves constructed from NADH solutions. The enzyme kinetics module of SigmaPlot 8.0 (SPSS Inc.) was used for regression analysis of the data, with the model for non-competitive inhibition to determine K_i for GSH.

For enzyme kinetics with multiple substrates, GSNO was added to a reaction mixture of different concentrations of a substrate alcohol (ethanol, octanol or HMGSH), 2.4 mM NAD^+ and 2.5 μg/ml (HMGSH) or 62.5 μg/ml (ethanol or octanol) of ADH3 in 0.1 M potassium phosphate (pH 7.5) at room temperature (22 °C). Both NADH and GSNO absorb at 340 nm, with molar absorption coefficients of 6220 and 840 $M^{-1} \cdot cm^{-1}$ respectively, but only NADH gives rise to fluorescence when excited at 340 nm. Reactions were monitored under equivalent conditions in a Hitachi U-3000 spectrophotometer at 340 nm and in a fluorescence spectrophotometer as described above. The molar absorptivity of GSNO was used to calculate reaction rates from the initial negative slopes in the absorbance measurements. For controls without GSNO, the molar absorptivity of NADH was used to calculate initial reaction rates. At the time scale monitored, no appreciable GSNO degradation was observed in controls without enzyme or in controls without NAD^+.

For kinetics with MGST1, enzyme activity was monitored at 30 °C by following the absorbance change at 340 nm in a reaction system containing 2 mM GSH, 0.5 mM CDNB (1-chloro-2,4-dinitrobenzene) and 2.5 % (v/v) ethanol as the solvent for CDNB, 0.1 M potassium phosphate (pH 6.5) and 0.1 % Triton X-100. Inhibitor (GSNO, glutathione sulfinamide, sulfinic acid and sulfonic acid) was added after determination of control activity. Glutathione sulfinamide and sulfinic acid were generated by the ADH3-mediated reaction and subsequently purified by FPLC-based separation (as described below), freeze-dried and dissolved in water. FPLC-based separation of a GSNO solution demonstrated minor contamination by glutathione sulfinamide, glutathione sulfinic acid, glutathione sulfonic acid and GSSG. Thus, prior to inhibition experiments, GSNO was similarly subjected to FPLC for purification. Inhibitor concentrations were determined by amino acid analysis (glutathione sulfinamide and sulfinic acid) or absorbance measurement at 340 nm (GSNO). Data were fitted by nonlinear regression with GraphPad Prism (GraphPad Software) using the model for one-site competition. IC_{50} values from two different experiments performed in triplicates agreed within ±20 %.

Product analysis of GSNO reduction

To analyse the products of GSNO reduction in the presence of GSH, 0.8 mM GSNO and 1 mM NADH were incubated at 37 °C with different concentrations of GSH (0, 1, 2 and 5 mM) in the absence and presence of 2.5 μg/ml ADH3. Reactions were protected from light and after the indicated reaction time (0, 10 or 60 min), crude reaction mixtures were directly analysed by ESI (electrospray ionization) MS or immediately resolved on a strong anion-exchange column (Resource Q, GE Healthcare), essentially as previously described [4]. ESI mass spectra of crude reaction mixtures, diluted 1:1 with 100 % (v/v) methanol and including 10 μM *S*-hexylglutathione as the internal standard, were collected on a Quattro Micro triple quadrupole mass spectrometer (Waters) fitted with the standard electrospray source. Samples were introduced at a flow rate of 10 μl/min using a syringe pump. The source temperature of the instrument was kept at 80 °C, the spray voltage was 1.7 kV and the cone voltage was varied between 20 and 40 V to obtain two different degrees of desolvation and

© The Authors Journal compilation © 2008 Biochemical Society

fragmentation. Notably, no acid (e.g. formic acid) was added to the sample for these experiments, because the sulfinamide was rapidly hydrolysed to the sulfinic acid at low pH. For FPLC separation of reaction products, the running buffers were 10 mM ammonium bicarbonate and 20 % acetonitrile (buffer A) and 1 M ammonium bicarbonate and 20 % acetonitrile (buffer B). Buffers A and B were de-aerated with nitrogen for 1 and 3–4 h, resulting in pH 9.0 and 9.5 respectively. The elution profile was monitored at 214 and 340 nm and semi-quantification was carried out by integration of the obtained reactant and product peaks at 214 and 340 nm (NADH and GSNO). Solutions of GSNO, GSH, GSSG and NADH with known concentrations (for GSNO and NADH determined by absorbance measurement at 340 nm) were used to calibrate peak intensities. For the commercially unavailable products glutathione sulfinamide and sulfinic acid, merely peak intensities were monitored. GSH_{unacc} (unaccounted [GSH]-scaffold) was calculated by subtracting the sum of GSH-derived products generated in the presence of ADH3 from the sum of all GSNO and GSH added in the beginning, for example for reactions after 10 min. GSX_0 and GSX_{10} are the measured concentrations after 0 and 10 min respectively:

$$GSH_{unacc} = (GSNO_0 + GSH_0) - [GSNO_{10} + GSH_{10} + 2(GSSG_{10} - GSSG_0)].$$

For confirmation of product identity, ESI mass spectra of product fractions were acquired using a Finnigan LCQ Deca ion-trap mass spectrometer equipped with an ESI source (Thermo Finnigan). Samples were diluted 1:1 with 100 % methanol and introduced into the instrument at a rate of 5 μl/min using a syringe pump via a silica capillary line. The capillary temperature was 200 °C and the spray voltage was 5 kV.

Concentrations of hydroxylamine were determined with a modified form of the colorimetric assay [28]. Aliquots (50 μl) of the reactions were removed before incubation as well as after 10 and 60 min incubation at 37 °C and diluted 5-fold with potassium phosphate buffer (pH 6.8). Then, 50 μl of 10 % (v/v) trichloroacetic acid and 500 μl of 1 % 8-hydroxyquinoline (prepared in 50 % ethanol) were added, followed by rapid mixing. A 500 μl portion of 1 M sodium carbonate was added, the solutions were mixed for 15–20 s and, after 2–3 min, the solutions were finally heated to 95 °C for 4 min. The solutions were then allowed to cool to room temperature, and the absorbance at 707 nm was measured after 60 min. Hydroxylamine concentrations were determined using standard curves constructed from hydroxylamine/hydrochloride solutions, also in the presence of 1, 2 and 5 mM GSH because thiols reduce the colour yield of the reaction (by 24 % for 1 mM GSH, 37 % for 2 mM GSH and 46 % for 5 mM GSH).

GSNO reduction in crude cell lysates

Liver and lung samples were from C57BL6 mice that had been anesthetized by an intraperitoneal injection of Avertin (2,2,2-tribromoethyl and tertiary amyl alcohol; 17 μl/g mice) [29]. Mice were housed and treated according to Swedish animal research regulations. All experiments were approved by the ethical committe of Karolinska Institutet. Samples were stored at −80 °C until they were thawed and homogenized in 10 mM Tris/HCl and 1 mM DTT (pH 8.0) with a Polytron homogenizer (Ultra-Turrax T25, Janke and Kunkel). The cell suspensions were sonicated and centrifuged at 48 000 ***g*** for 60 min at 4 °C. Low-molecular-mass compounds were removed from the supernatant using a PD-10 column (GE Healthcare). Protein content of the cell lysates was determined using the Bradford [29a] method (Bio-Rad). Reactions with 0.5 mg/ml protein from liver lysate for product analysis were performed as described above. For GSNO reduction in the presence of HMGSH/ethanol and NAD^+, reaction mixtures containing 0.5 mg/ml (liver) or 0.25 mg/ml (lung) protein and variably 1 mM GSNO, 1 mM GSH, 1 mM formaldehyde and 2.4 mM NAD^+ were monitored at 340 nm at 37 °C for 10 min. Reaction rates were determined as described above for reactions with purified ADH3.

Cell culture, formaldehyde exposure and cell lysis

The buccal carcinoma cell line SqCC/Y1 (passages 157–159) was cultured in EMHA (epithelial medium with high levels of amino acids) under serum-free conditions until 90–100 % confluency was reached, as previously described [30]. Mock treatment and exposure to 1, 2, 5 and 10 mM formaldehyde were for 1 h in a chemically defined variant of EMHA without pituitary extract and cysteine [31]. After exposure, cells were washed twice with cold PBS on ice, scraped off the culture plate into a small volume of PBS, counted in a Neubauer cytometer and shortly spun down. After that, the cells were immediately snap-frozen and stored in liquid nitrogen until they were finally resuspended in Griess lysis buffer [50 mM Tris/HCl, pH 8.0, 150 mM NaCl, 5 mM KCl, 1 % Nonidet P40, 1 mM bathocuproinedisulfonic acid, 1 mM DTPA (diethylenetriaminepenta-acetic acid), 10 mM NEM (*N*-ethylmaleimide) and one Complete™ protease inhibitor cocktail tablet (Roche)] and lysed for 15 min on ice. Lysis was followed by 10 min centrifugation at 15 000 ***g*** at 4 °C. Protein content of the cell lysates was determined using the Bradford [29a] method (Bio-Rad). Exposures to 1–10 mM formaldehyde did not significantly affect the measured total protein content per cell.

Quantification of intracellular nitrosothiols by the Saville–Griess assay

A 25 μl portion of cell lysate corresponding to approx. 200 μg of total protein content was incubated with 1 % sulfanilamide and 0.1 % *N*-(1-naphthyl)ethylenediamine in the presence or absence of 2.5 mM $CuCl_2$ for 15 min, and the nitrosothiol content was measured photometrically at 540 nm. The amount was calculated using a standard curve obtained with GSNO solutions of known concentration. The results are based on three to four experiments and statistical significance was determined using a two-tailed, unpaired Student's *t* test.

RESULTS

GSNO increased the rate of ADH3-mediated oxidation of HMGSH and other alcohols

Reaction rates of octanol, ethanol and HMGSH oxidation were studied in the absence and presence of GSNO by absorption and fluorescence spectroscopy. In the absence of GSNO, initial octanol oxidation rates were determined using the molar absorption coefficient of NADH (Figure 1A). In the presence of GSNO, no fluorescence emission, hence no net NADH production, was observed in the first section of the reaction and thus the concurrent negative slope monitored at 340 nm corresponded to the decrease of GSNO in the reaction mixture and could be used to determine reaction rates using the molar absorption coefficient (ε) of GSNO. The obtained rates for the oxidation of three different substrates, i.e. octanol, ethanol and HMGSH, in the absence and presence of GSNO showed a uniform pattern (Figures 1B–1D): in the presence of GSNO, reaction rates were considerably increased, notably up to 8-fold for the substrate pair HMGSH/GSNO (Figure 1D). Similar reactions were performed for the substrate

© The Authors Journal compilation © 2008 Biochemical Society

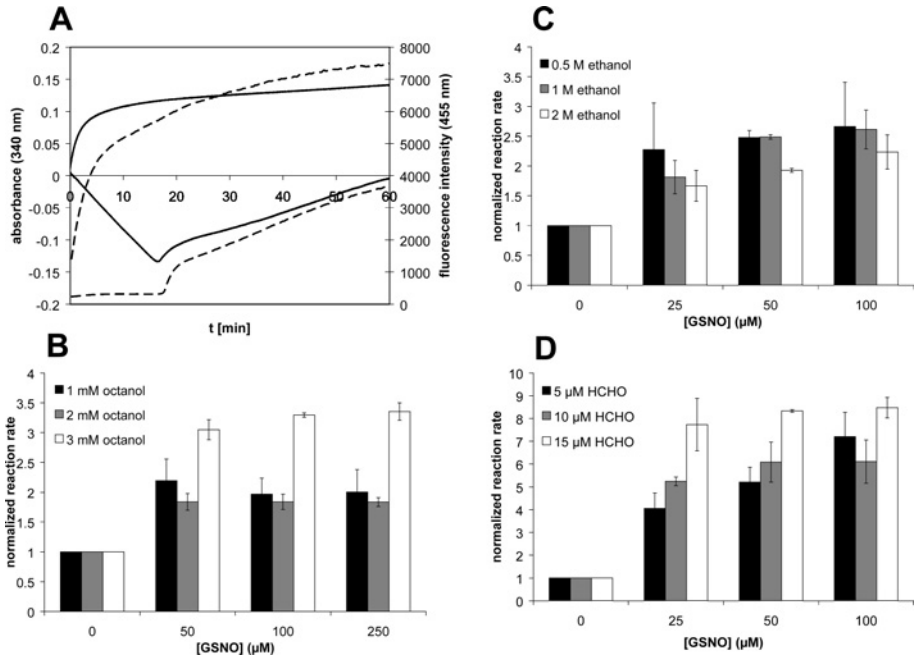

Figure 1 ADH3-mediated alcohol oxidation in the presence of GSNO

(**A**) Measurement principle: ADH3-catalysed octanol oxidation in the presence and absence of 250 μM GSNO. Reactions were carried out in 0.1 M potassium phosphate (pH 7.5) containing 2.4 mM NAD^+, 2.0 mM octanol and 62.5 μg/ml ADH3 in the presence (lower curves) and absence (upper curves) of 250 μM GSNO. Solid lines show reactions monitored by following the absorbance at 340 nm. Dashed lines show reactions monitored by following NADH-specific fluorescence emission at 455 nm with 340 nm as the λ_{ex}. In the presence of GSNO, the initial negative slope coincides with the absence of net NADH production. (**B**–**D**) Normalized rates of alcohol oxidation in the absence (rate = 1) and presence of GSNO for the substrates (**B**) octanol, (**C**) ethanol and (**D**) formaldehyde (in the form of HMGSH). For reactions with formaldehyde, the ADH3 concentration was 2.5 μg/ml and reaction mixtures also contained 1 mM GSH. Results are presented as means ± S.D. for at least two independent experiments.

Table 1 Reaction rates of GSNO conversion and formaldehyde (HCHO) or ethanol oxidation in crude mouse liver and lung lysates

All reactions were carried out at 37 °C in 0.1 M potassium phosphate (pH 7.5) containing 2.4 mM NAD^+ and 0.5 mg/ml (liver lysate) or 0.25 mg/ml protein (lung lysate). Different combinations of substrates (1 mM each) were added as indicated. Reactions were monitored by following the absorbance at 340 nm. Results are expressed as micromoles of NADH formed or, in the absence of net NADH formation, micromoles of GSNO degraded/min per g of total protein and shown as means ± S.D. from two experiments with one lysate. For reactions including GSNO with or without GSH, background from controls without cell lysate was subtracted.

Substrates				Reaction rate (μmol · min^{-1} · g^{-1})	
				Liver lysate	Lung lysate
HCHO	NAD^+			3.2 ± 0.5*	0.33 ± 0.12*
HCHO	NAD^+	GSH		13 ± 0.2*	2.2 ± 0.04*
HCHO	NAD^+		GSNO	14 ± 5†	1.7 ± 0.16†
HCHO	NAD^+	GSH	GSNO	310 ± 20†	55 ± 0.4†
	NAD^+	GSH	GSNO	n.s.‡	n.s.‡
		GSH	GSNO	n.s.‡	n.s.‡
			GSNO	n.s.‡	n.s.‡
Ethanol	NAD^+			4.9 ± 0.2*	0.75 ± 0.12*
Ethanol	NAD^+		GSNO	5.0 ± 1.2†	0.36 ± 0.03*

*Net NADH production observed; rates were calculated using the molar absorptivity of NADH.
†No initial net NADH production; rates were calculated using the molar absorptivity of GSNO.
‡n.s., no significant activity in comparison with the control without lysate.

pair HMGSH/GSNO with crude cell lysates from mouse liver and mouse lung (Table 1). Oxidation of formaldehyde was observed in the absence and presence of GSH, but the presence of GSH, allowing HMGSH formation, increased the reaction rate approx. 4-fold for liver and 7-fold for lung lysate. Adding GSNO to these reaction mixtures caused a further rate increase, which was similar for both types of crude cell lysates. Reactions without added GSH were accelerated approx. 5-fold, whereas reactions including GSH were accelerated approx. 25-fold. A different pattern was observed for ethanol: with liver lysate, similarly, no net NADH production was observed, but reaction rates were equal in the absence and presence of GSNO. With lung lysate, net NADH production was decreased to approx. 50 % in the presence of GSNO. Experiments with independently prepared lysates yielded similar results and the addition of metal chelators, e.g. neocuproine, a Cu(I)-chelator [32], and DTPA [33], did not significantly change the rate of enzyme-independent GSNO decomposition in the presence of GSH.

Formaldehyde reduced intracellular S-NO content

To assess whether formaldehyde exposure influences the levels of intracellular S-NOs in intact cells, the buccal carcinoma cell line SqCC/Y1 was exposed to various concentrations of formaldehyde for 1 h. Subsequent S-NO quantification revealed a trend towards decreased intracellular S-NO levels after exposure to 1–5 mM formaldehyde, which was statistically significant for 5 mM (Figure 2). This effect was partly counteracted at a concentration of 10 mM formaldehyde.

Steady-state kinetics for HMGSH oxidation and GSNO reduction

Steady-state kinetics for ADH3 with HMGSH and GSNO as substrates exhibited a K_m value for HMGSH that was approx. 100-fold lower than the one for GSNO, as recorded by fluorescence spectroscopy (Table 2). In contrast, k_{cat} was 10-fold higher for GSNO reduction and, consequently, the catalytic efficiency was

© The Authors Journal compilation © 2008 Biochemical Society

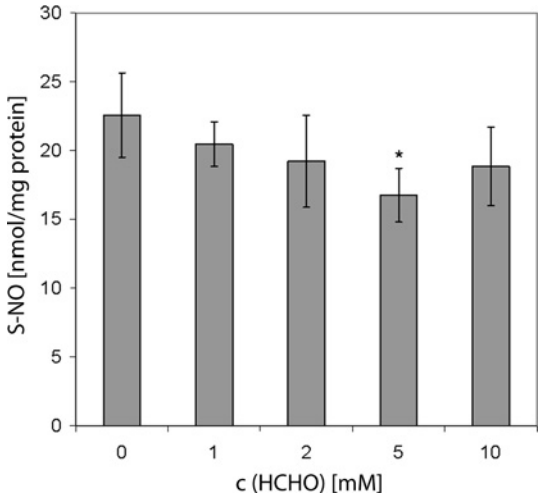

Figure 2 S-NO content in SqCC/Y1 cells in response to formaldehyde exposure

Cells were exposed to the indicated concentrations of formaldehyde for 1 h. S-NO content was measured using the Saville–Griess assay as described in the Experimental section. Results are presented as means ± S.D. for at least three independent experiments. Statistical significance was determined using a Student's *t* test; $^{*}P < 0.05$ compared with mock-treated control.

Table 2 Steady-state kinetic parameters for HMGSH oxidation/GSNO reduction

K_m, k_{cat} (per subunit, 40 kDa) and K_i values were obtained from initial velocity experiments at 25 °C monitored by fluorescence spectrophotometry and are given as means ± S.D. for at least three independent experiments. NAD^+ and NADH concentrations were fixed at 2.4 and 0.1 mM respectively. n.d., not determined.

	HMGSH	GSNO
K_m (μM)	0.12 ± 0.02	11.1 ± 2.9
k_{cat} (min^{-1})	150 ± 10	1200 ± 150
k_{cat}/K_m ($min^{-1} \cdot \mu M^{-1}$)	1300 ± 210	110 ± 30
K_i (GSH) (mM)	n.d.	14.3 ± 1.3

approx. 10-fold higher for HMGSH oxidation than for GSNO reduction. GSH inhibited ADH3-mediated GSNO reduction at millimolar concentrations and the model for non-competitive inhibition yielded a K_i of 14.3 mM.

Product formation after GSNO reduction responded to GSH levels

Products of GSNO reduction in the absence and presence of GSH were initially analysed by performing ESI MS of crude reaction mixtures after incubation with or without ADH3, in the presence of 0–5 mM GSH. Using this approach, glutathione sulfinamide [339 a.m.u. (atomic mass units)] and sulfinic acid (340 a.m.u.) were detected at all GSH concentrations, but only in mixtures containing ADH3 (Figure 3). Overall, the spectra were characterized by peak clusters of +22 a.m.u., e.g. 339, 361 and 383 a.m.u., which were tentatively assigned as the protonated and singly/doubly sodiated species of one compound. This was partly confirmed by cone-voltage collision-induced dissociation; for instance, peaks at 361 and 414 a.m.u. were identified as singly sodiated adducts of glutathione sulfinamide (339 + 22 a.m.u.) and the internal standard *S*-hexylglutathione (392 + 22 a.m.u.) respectively (results not shown). Apart from glutathione sulfinamide, glutathione sulfinic acid and GSSG, no other reaction products, e.g. the suggested intermediate *S*-aminoglutathione (323 a.m.u.) [21], were detected.

For quantification, reaction products were separated on a strong anion-exchange column. An elution profile of reactants and products of GSNO reduction in the presence of 1 mM GSH showed that reactant and product peaks were sufficiently well separated (Figure 4). The results for controls without ADH3 (Table 3) demonstrate that GSH and GSNO are slowly consumed in a non-enzymatic reaction giving rise to GSSG as the major product after 60 min. Here, all initially included [GSH]-scaffold is accounted for by the measured products within a variation of 10 %. Addition of neocuproine did not change product yields in the controls. In reaction mixtures containing ADH3, at least 80 % of the initial GSNO were consumed after 10 min and associated qualitatively with the formation of glutathione sulfinamide and, in the presence of GSH, a fast consumption of GSH in favour of GSSG, particularly in reactions including 1 and 2 mM GSH (Tables 3 and 4). Yields of glutathione sulfinamide were only slightly decreased in the presence of 1 and 2 mM GSH, whereas a drastic decrease was observed in the presence of 5 mM GSH. Glutathione sulfinic acid was mainly observed in reactions without GSH, where levels increased with time (Table 4). Some glutathione sulfinic acid was also detected in the presence of 1 and 2 mM GSH after 60 min. Hydroxylamine formation was increasingly detected in reactions containing 2 and 5 mM GSH and correlated with a significant decrease in glutathione sulfinamide, particularly for the reaction containing 5 mM GSH. When crude mouse liver lysate was added to a reaction mixture of GSNO and NADH without GSH, glutathione sulfinamide and glutathione sulfinic acid remained the major products identified by FPLC separation and tandem MS. With the applied methods, no further metabolites of the sulfinamide and the sulfinic acid were observed after 60 min incubation with crude lysate. Moreover, adding GSH to the reaction resulted in a comparable product yield shift from the sulfinamide towards GSSG as described for purified ADH3 (results not shown).

Glutathione sulfinamide and sulfinic acid inhibited MGST1

GSNO, glutathione sulfinamide and glutathione sulfinic acid were tested as inhibitors for purified rat MGST1 and were found to inhibit the enzyme with IC_{50} values ranging from 520 to 22 μM (Table 5). Among the ADH3 products, glutathione sulfinic acid was the strongest inhibitor, close to the established GST inhibitor glutathione sulfonic acid.

DISCUSSION

Human ADH3 was investigated in its dual function as GSNOR and GSH-dependent formaldehyde dehydrogenase. In the presence of NAD^+ and initial absence of NADH, ADH3-mediated GSNO reduction was triggered by the presence of formaldehyde (in the form of HMGSH) and other substrates with concomitant reduction of NAD^+. At the same time, oxidation of HMGSH was promoted by the presence of GSNO. This effect was considerably more pronounced when crude protein extracts were used instead of purified ADH3. Exposure of cultured cells to 5 mM formaldehyde significantly altered intracellular S-NO content. Final product formation after ADH3-mediated GSNO reduction responded to changes in GSH concentrations. The products formed at lower GSH/GSNO ratios, glutathione sulfinamide and glutathione sulfinic acid, inhibited MGST up to 50 times stronger than GSNO.

For better sensitivity, steady-state kinetics was studied by fluorescence spectroscopy instead of the more commonly used absorbance spectroscopy. This allows for monitoring enzyme kinetics using considerably lower enzyme and substrate concentrations. With substrate concentrations ranging from 0.07 to

© The Authors Journal compilation © 2008 Biochemical Society

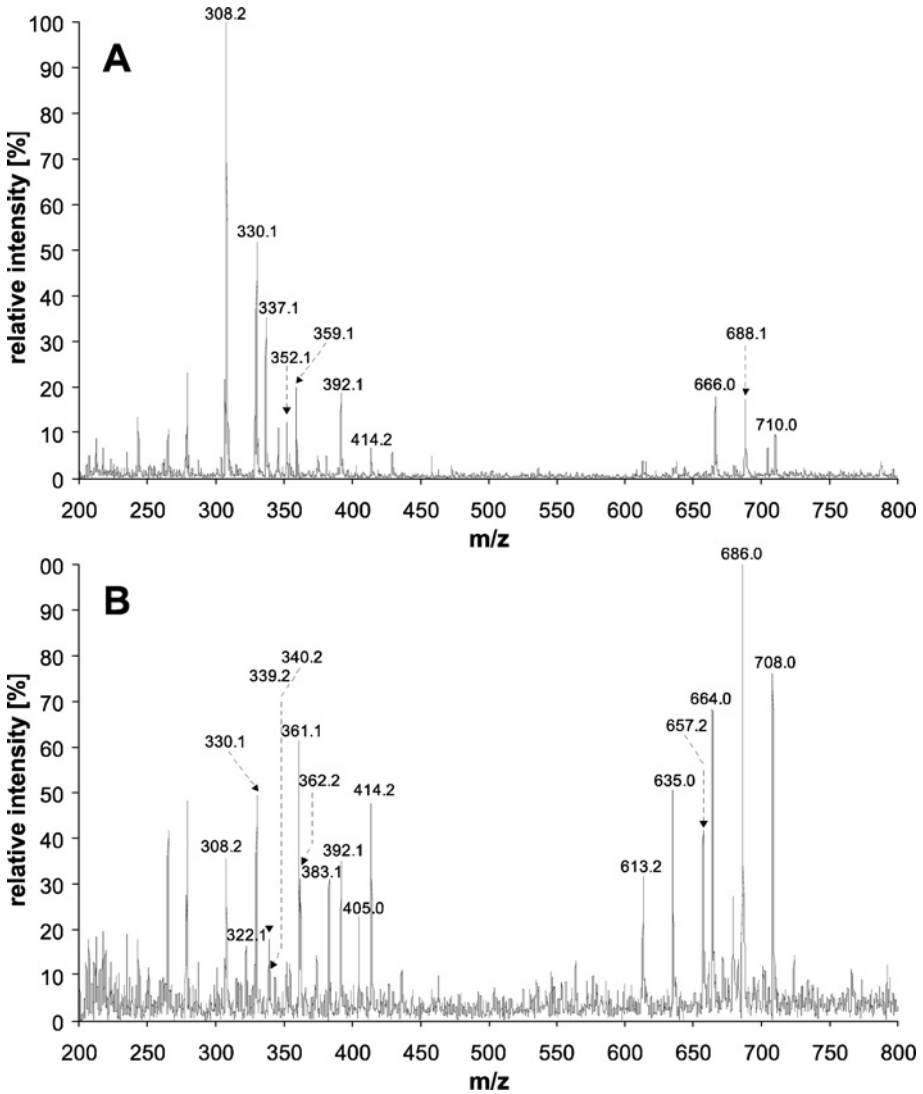

Figure 3 ESI mass spectra of crude reaction mixtures in the absence (A) and presence (B) of ADH3 after 10 min reaction time at 37 °C

Reaction mixtures containing 0.8 mM GSNO, 1 mM NADH and 1 mM GSH were incubated for 10 min in the absence and presence of 2.5 μg/ml ADH3. Peaks including protonated and most likely singly/doubly sodiated species (clusters of +22 a.m.u.) were assigned as follows: GSH: 308.2, 330.1, 352.1; GSNO: 337.1, 359.2; *S*-hexylglutathione (internal standard): 392.1, 414.2; GSSG: 613.2, 635.0, 657.2; NADH: 666.0, 688.1, 710.0; $GSONH_2$: 339.2, 361.1, 383.1, 405.0; GSO_2H: 340.2, 362.2; NAD^+: 664.0, 686.0, 708.0. The peak at 322.1 corresponds to the fragment ion of $GSONH_2$ and GSO_2H (cf. Figure 5).

1.44 μM and an enzyme concentration of 6.25 nM (calculated per monomer), we determined the K_m of ADH3 for HMGSH to be 0.12 μM. This value is approx. 5–10-fold lower than previously determined values, whereas the K_m for GSNO and the obtained k_{cat} values were mostly consistent with previous results for the human enzyme (Table 6) [4,27,34–36]. Thus the K_m for HMGSH is the determining factor to explain why the enzyme's efficiency, illustrated by k_{cat}/K_m, is highest for HMGSH in the present study.

The cytosolic free NAD^+/NADH ratio is favourable for oxidative reactions [13] and, hence, the incidence of GSNO reduction by ADH3 *in vivo* is strongly governed by NADH accessibility. Oxidation of HMGSH and other alcohols by ADH3 yields NADH, but the simultaneous presence of GSNO, HMGSH and both oxidized and reduced cofactors could conceivably lead to the formation of ternary dead-end inhibitory complexes, which would slow down the overall reaction. In contrast, the present study showed that the presence of GSNO accelerated the oxidation of HMGSH and other alcohols under concomitant reduction of GSNO (Figure 1). This effect is probably due to circumvention of cofactor release, a step that is partially rate-determining [34]. Similar experiments using crude lysates showed an even more drastic increase in HMGSH oxidation rate (>20-fold) when GSNO was added (Table 1). Again, this finding can be explained by circumvention of cofactor release, which gains importance in a more complex context including other NAD^+/NADH-scavenging enzymes present in the cell extracts. The reaction rate increases in reaction mixtures containing formaldehyde and GSNO without added GSH are probably due to contamination of GSNO preparations with GSSG (~10 %, see controls in the absence of GSH, Table 3), rapidly reduced to GSH by glutathione reductase, which ultimately allows some HMGSH formation.

When only adding the oxidized cofactor (and thus, to some extent, mimicking the high cellular NAD^+/NADH ratio), no significant enzymatic GSNO-reducing activity was observed in the absence of formaldehyde (Table 1). These findings suggest that out of all of the so far identified potential GSNO-degrading

© The Authors Journal compilation © 2008 Biochemical Society

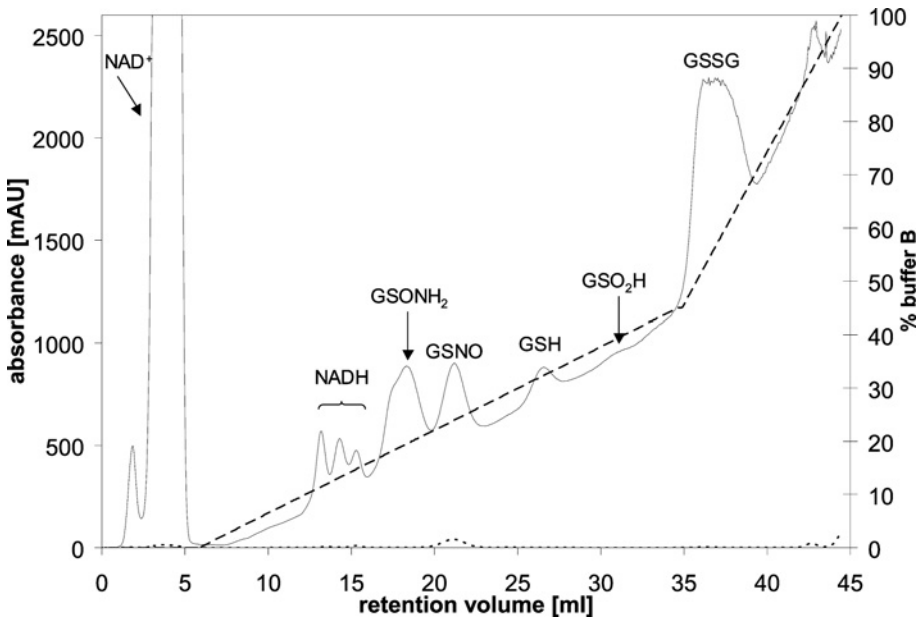

Figure 4 Separation of reactants and products of ADH3-mediated reduction of GSNO in the presence of GSH

Reaction mixtures containing 0.8 mM GSNO, 1 mM NADH and 1 mM GSH were incubated for 10 min including 2.5 μg/ml ADH3. The reaction mixtures were resolved on a strong anion-exchange column with a linear gradient from 10 to 450 mM ammonium bicarbonate with 20 % acetonitrile (dashed line). The elution profile was monitored at 214 nm (solid line) and 340 nm (dotted line). Product identities were confirmed by ESI tandem MS. The leftmost of the three peaks depicted as NADH yielded an *m*/*z* value of 665 a.m.u. instead of 666 a.m.u. and did not absorb at 340 nm. $GSONH_2$, glutathione sulfinamide, GSO_2H, glutathione sulfinic acid, mAU, milliabsorbance units.

Table 3 Determination of reactant and product yields of GSNO reduction in response to GSH concentrations

Yields of GSH, GSSG and hydroxylamine (NH_2OH) in reaction mixtures containing GSNO, NADH and different concentrations of GSH, in the absence and presence of ADH3. Results from at least two independent experiments are presented as means ± S.D.

	Concentration (mM)							
	− ADH3				+ ADH3			
t (min)	No GSH	1 mM GSH	2 mM GSH	5 mM GSH	No GSH	1 mM GSH	2 mM GSH	5 mM GSH
GSNO*								
0	0.79 ± 0.08	0.78 ± 0.01	0.72 ± 0.02	0.75 ± 0.01	–	–	–	–
10	0.80 ± 0.13	0.77 ± 0.05	0.68 ± 0.01	0.68 ± 0.01	0.09 ± 0.06	< 0.01	< 0.01	0.17 ± 0.01
60	0.76 ± 0.11	0.56 ± 0.05	0.50 ± 0.03	0.44 ± 0.07	0.09 ± 0.06	< 0.01	< 0.01	< 0.01
NADH*								
0	0.91 ± 0.09	0.87 ± 0.04	0.84 ± 0.01	0.89 ± 0.06	–	–	–	–
10	0.89 ± 0.12	0.88 ± 0.12	0.83 ± 0.01	0.87 ± 0.06	< 0.01	< 0.01	0.04 ± 0.05	0.31 ± 0.09
60	0.84 ± 0.12	0.75 ± 0.01	0.74 ± 0.01	0.73 ± 0.01	< 0.01	< 0.01	0.06 ± 0.03	0.07 ± 0.06
GSH*								
0	< 0.01	1.13 ± 0.03	2.11 ± 0.04	4.98 ± 0.32	–	–	–	–
10	< 0.01	1.11 ± 0.02	2.09 ± 0.02	4.75 ± 0.24	< 0.01	0.07 ± 0.04	1.22 ± 0.03	4.81 ± 0.34
60	< 0.01	0.87 ± 0.11	1.93 ± 0.09	4.66 ± 0.18	< 0.01	0.03 ± 0.04	1.14 ± 0.05	4.80 ± 0.23
GSSG*								
0	0.08 ± 0.05	0.16 ± 0.05	0.24 ± 0.01	0.32 ± 0.03	–	–	–	–
10	0.11 ± 0.05	0.21 ± 0.03	0.26 ± 0.04	0.36 ± 0.01	0.12 ± 0.02	0.68 ± 0.08	0.73 ± 0.10	0.46 ± 0.06
60	0.09 ± 0.04	0.32 ± 0.06	0.31 ± 0.06	0.52 ± 0.01	0.15 ± 0.01	0.78 ± 0.08	0.80 ± 0.08	0.60 ± 0.03
NH_2OH†								
0	< 0.01	< 0.01	< 0.01	< 0.01	–	–	–	–
10	< 0.01	< 0.01	< 0.01	< 0.01	< 0.01	< 0.01	0.042 ± 0.005	0.091 ± 0.019
60	< 0.01	< 0.01	< 0.01	< 0.01	< 0.01	< 0.01	0.037 ± 0.007	0.084 ± 0.024
GSH_{unacc}‡								
0	n.a.§	n.a.§	n.a.§	n.a.§	–	–	–	–
10	n.a.§	n.a.§	n.a.§	n.a.§	0.62	0.80	0.63	0.47
60	n.a.§	n.a.§	n.a.§	n.a.§	0.56	0.67	0.57	0.37

*Quantification of GSNO, GSH, GSSG and NADH was performed by integration of the obtained product peaks at 340 nm (NADH, GSNO) or 214 nm (GSH, GSSG) after separation on a strong anion-exchange column (cf. Figure 4).

†NH_2OH was trapped as quinoline oxime and determined colorimetrically as described in the Experimental section.

‡Unaccounted [GSH]-scaffold (GSH_{unacc}) was calculated as described in the Experimental section.

§n.a., not applicable: all the [GSH]-scaffold in controls without ADH3 was accounted for within a variation of 10 %.

© The Authors Journal compilation © 2008 Biochemical Society

Table 4 Peak areas from FPLC chromatograms reflecting glutathione sulfinamide ($GSONH_2$) and sulfinic acid (GSO_2H) yields after GSNO reduction, in response to GSH concentration

Peak areas ($mAU_{214} \times ml$) correspond to $GSONH_2$ and GSO_2H yield after separation on a strong anion-exchange column (cf. Figure 4), in the absence and presence of ADH3 and different concentrations of GSH. Results from at least two independent experiments are presented as means ± S.D. Abbreviation: mAU, milliabsorbance units.

	Concentration (mM)							
	− ADH3				+ ADH3			
t (min)	No GSH	1 mM GSH	2 mM GSH	5 mM GSH	No GSH	1 mM GSH	2 mM GSH	5 mM GSH
$GSONH_2$								
0	174 ± 15	163 ± 30	114 ± 7	136 ± 25	–	–	–	–
10	199 ± 21	182 ± 28	152 ± 41	129 ± 65	1019 ± 25	994 ± 43	937 ± 62	253 ± 12
60	195 ± 4	221 ± 56	198 ± 56	202 ± 56	989 ± 7	991 ± 82	969 ± 123	336 ± 19
GSO_2H								
0	n.d.*	n.d.*	n.d.*	n.d.*	–	–	–	–
10	n.d.*	n.d.*	n.d.*	n.d.*	243 ± 17	n.d.*	n.d.*	n.d.*
60	12 ± 11	n.d.*	n.d.*	n.d.*	391 ± 13	40 ± 10	37 ± 10	n.d.*

*n.d., not detected.

Table 5 Inhibition of MGST1 activity by GSNO and products of GSNO reduction in comparison with the known inhibitor glutathione sulfonic acid (GSO_3H)

Enzyme activity was monitored at 30 °C after an absorbance change at 340 nm in solutions containing 2 mM GSH and 0.5 mM CDNB. Inhibitor concentrations were determined by amino acid analysis [glutathione sulfinamide ($GSONH_2$) and sulfinic acid (GSO_2H)] or absorbance measurement at 340 nm (GSNO). Results are from triplicate measurements and are presented as means ± S.E.M.

	IC_{50} (μM)
GSNO	520 ± 15
$GSONH_2$	48 ± 1.0
GSO_2H	22 ± 0.2
GSO_3H	5.3 ± 0.3

enzymes including Cu/Zn superoxide dismutase [37], glutathione peroxidase [38], the thioredoxin system [39] and xanthine oxidase [40], ADH3 is the main enzyme responsible for GSNO degradation in liver and lung once NADH becomes available. Furthermore, NADH formed by ADH3-mediated alcohol oxidation is likely to trigger fast GSNO reduction against the usually high cytosolic NAD^+/NADH ratio because the reduced cofactor remains bound to the enzyme.

The importance of the cofactor recycling being enzyme-bound is illustrated by the fact that ethanol, an ADH3 substrate only at molar concentrations [36] (cf. Figure 1C), does not trigger a reaction rate increase at millimolar concentrations where other ADHs metabolize ethanol much more efficiently than ADH3 [2]. The resulting increase in available NADH still triggers GSNO reduction in liver lysate and probably also in lung lysate where the decrease in absorbance due to GSNO reduction is probably masked by residual NADH production. However, the overall reaction rate is not increased in this case, where alcohol oxidation and GSNO reduction are not constrained to the same enzyme. Instead, the GSNO reduction rate appears to be limited by the rate of free NADH production after alcohol oxidation. Overall, the results suggest that, through the dual function of ADH3 as formaldehyde dehydrogenase and GSNOR, formaldehyde can cause rapid GSNO depletion by enzyme-bound cofactor recycling.

The suggested mechanism, enzyme-bound cofactor recycling facilitated by the presence of a substrate for the reverse reaction, might provide a more general mechanism to overcome unfavourable cofactor ratios. In fact, a stimulation of reduction by ADH has previously been reported for the substrate couple ethanol/cyclohexanone in rat hepatocytes [41]. The prerequisites for the catalytic rate to increase by enzyme-bound cofactor recycling must be the following: first, the reaction rate of the forward reaction is determined by cofactor binding/release; secondly, association of the substrate for the reverse reaction, subsequent hydride transfer and dissociation of the product are faster than cofactor binding/release accompanying the first reaction. Our results suggest that this is the case for ADH3-mediated GSNO reduction during HMGSH oxidation. On the contrary, in the

Table 6 A comparison of the steady-state kinetic parameters reported so far for GSNO reduction and HMGSH oxidation by human ADH3

Values were determined using different substrate ranges, but otherwise similar experimental conditions, in the presence of the respective cofactor in excess, at 25 °C (except for HMGSH kinetics from [34], 30 °C) and pH 7.5 or 8.0. n.d., not detected.

HMGSH			GSNO			
K_m (μM)	k^*_{cat} (min^{-1})	k_{cat}/K^*_m ($min^{-1} \cdot \mu M^{-1}$)	K_m (μM)	k^*_{cat} (min^{-1})	k_{cat}/K^*_m ($min^{-1} \cdot \mu M^{-1}$)	Reference
0.12	150	1300	11.1	1200	110	The present study
2	115	58	27	2400	90	[4]
1.7	150	90	4.8	1760	370	[34]
1.4	160†	115†	27	6000†	220	[35]
0.63	56	89	n.d.	n.d.	n.d.	[36]
0.8	62	78	n.d.	n.d.	n.d.	[27]

*All values are calculated with the molecular mass of an ADH3 monomer (40 000 Da).
†The value was originally calculated with the molecular mass of an ADH3 dimer (80 000 Da) and was recalculated with 40 000 Da for comparison.

© The Authors Journal compilation © 2008 Biochemical Society

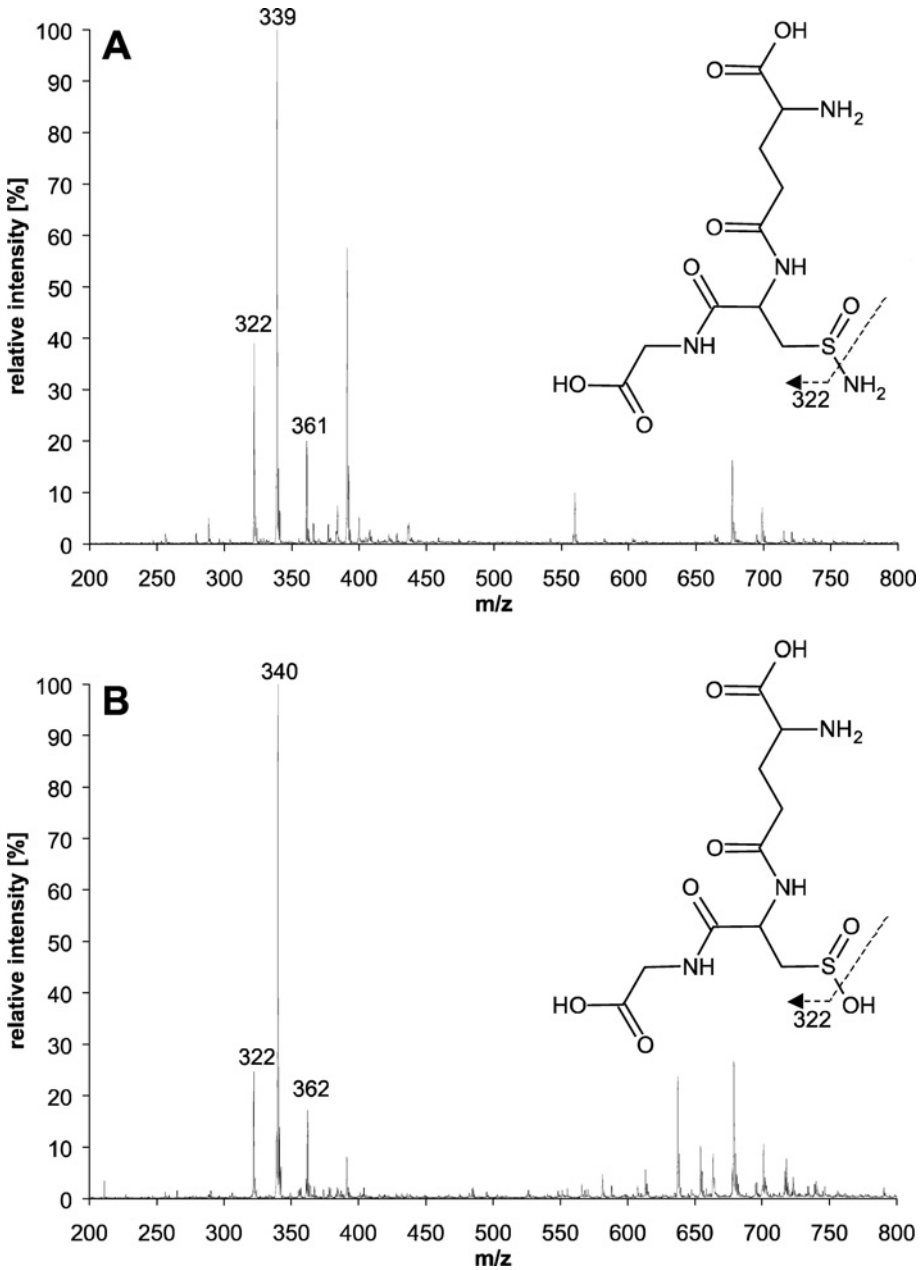

Figure 5 ESI mass spectra of the reaction products glutathione sulfinamide (A) (339 a.m.u.) and glutathione sulfinic acid (B) (340 a.m.u.), demonstrating their identity and purity, as obtained by FPLC

The peaks at 322 a.m.u. correspond to the fragment ion resulting from cleavage behind the sulfoxy group (depicted with arrows) in both compounds. The peaks at 361 and 362 a.m.u. correspond to sodium adducts of $GSONH_2$ and GSO_2H respectively. Notably, for $GSONH_2$, no contamination by glutathione sulfinic acid and, for both, no contamination by glutathione sulfonic acid (356 a.m.u.) was observed.

presence of NADH, even with HMGSH concentrations exceeding GSNO concentrations by a factor of 200, we were not able to establish conditions where no net NADH consumption was observed (results not shown). Thus formaldehyde did not increase the GSNO reduction rate in the presence of GSH and NADH, a result that indicates that one of the above mentioned prerequisites is not fulfilled.

Previous reports emphasize the importance of compartmentalization in NO signalling, consistent with the highly diffusible and short-lived character of NO [42,43]. Yet, as a relatively stable storage form of NO, GSNO might be less dependent on specific cellular location to exert its functions. ADH3 has been shown to be located throughout the nucleus and cytoplasm [35]. Thus formaldehyde might lead to depletion of GSNO and, consequently, total cellular protein S-NO levels. In addition, ADH3 levels are increased in allergen-challenged airways [10]; the same mechanism might thus affect the regulation of airway responsivity, where GSNO functions as an endogenous bronchodilator, whereas formaldehyde causes bronchoconstriction and has been correlated with exacerbation of asthma symptoms [10,19,44–46]. In agreement, application of the SqCC/Y1 cell line with well-documented ADH3 activity [3] shows that a relatively

© The Authors Journal compilation © 2008 Biochemical Society

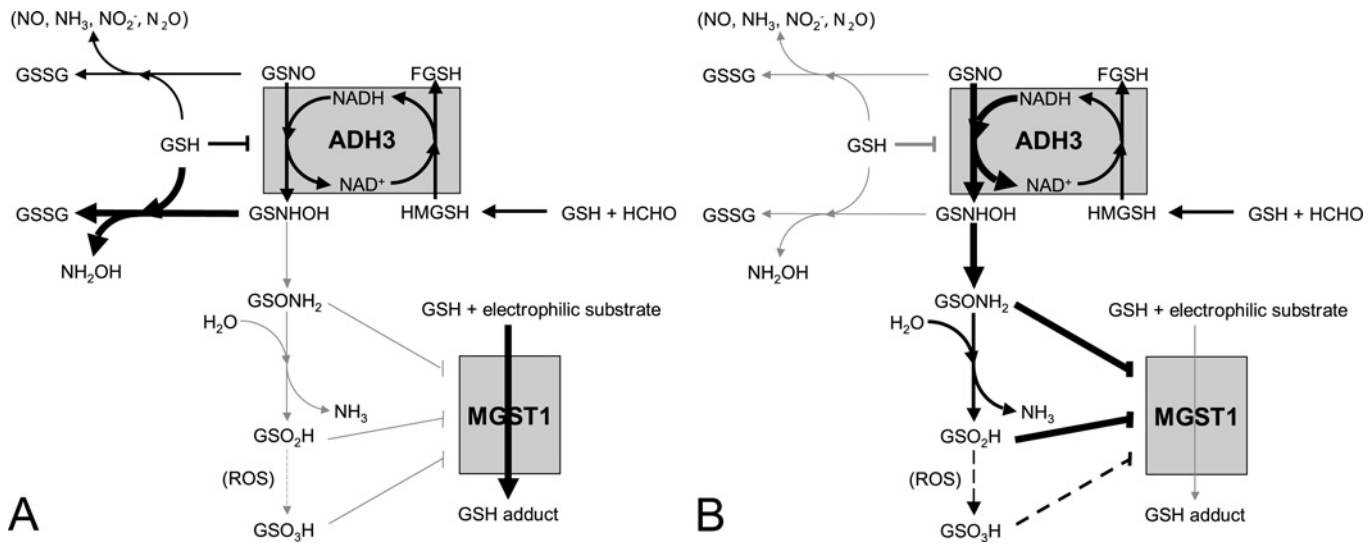

Figure 6 Model for product formation of ADH3-mediated GSNO reduction responding to local GSH concentration

(**A**) Abundant GSH: GSH at millimolar concentrations decreases the rate of ADH3-mediated GSNO reduction. GSNO reduced by ADH3 to the intermediate *S*-(*N*-hydroxyamino)glutathione is intercepted by GSH to yield GSSG and NH_2OH. No inhibitors of MGST1 are formed. Some GSNO is converted in a slow non-enzymatic reaction to yield GSSG and a variety of nitric species, dependent on local oxygen concentrations [32,51]. (**B**) Severe GSH depletion: ADH3-mediated GSNO reduction is fast and the intermediate *S*-(*N*-hydroxyamino)glutathione can be spontaneously rearranged to the glutathione sulfinamide. Glutathione sulfinamide is partly hydrolysed to sulfinic acid, which is likely to be oxidized to glutathione sulfonic acid under oxidative stress [ROS (reactive oxygen species)]. The three product species generated under GSH depletion, glutathione sulfinamide, sulfinic acid and sulfonic acid, increasingly inhibit MGST1, an enzyme that consumes GSH in detoxification of electrophilic substrates. Invariably, NADH for GSNO reduction can be provided by oxidative ADH3 pathways, e.g. by oxidation of the glutathione adduct of formaldehyde, HMGSH.

short formaldehyde exposure (1 h) at concentrations from 1 to 5 mM indeed results in a trend towards decreased S-NO content in cultured cells with a maximal effect at 5 mM. Although suggestive in nature, this observation does not prove an ADH3-mediated effect and future studies using gene silencing or knockout systems will be necessary to elucidate whether the mechanism proposed above is functional *in vivo*. The formaldehyde effect appears to be partly counteracted at a concentration of 10 mM, which could be explained by well-known cytotoxic effects of formaldehyde: for instance, an increase in protein S-nitrosation could be the result of GSH depletion after formaldehyde assimilation and HMGSH formation [5,47], but also the result of an increase in free cytosolic Ca^{2+} levels which possibly induces NO synthase activity [48,49].

Previous reports have shown that the product of ADH3-mediated GSNO reduction *in vitro*, in the absence of GSH, is glutathione sulfinamide [4,20]. However, controversial results have been reported for reaction products in the presence of GSH [20,21]. GSH normally exists in millimolar concentrations in mammalian cells, whereas reported GSNO concentrations are in the micromolar range [46,50]. Thus our results imply that the most likely physiological product under normal cellular redox conditions is GSSG, as the product of the fast ADH3-catalysed reaction as well as of the slow non-enzymatic reaction between GSNO and GSH (Table 3) [51,52]. This is in agreement with another study that showed that the presence of 5 mM GSH decreased glutathione sulfinamide yields in favour of GSSG and hydroxylamine [20]. Thus, consistent with the inhibitory effects observed in steady-state kinetics experiments (Table 2), typical cellular GSH levels will decrease the rate of enzyme-catalysed GSNO reduction, facilitate the quantitative interception of the intermediate semimercaptal by GSH to form GSSG and preclude the spontaneous rearrangement to the sulfinamide (Figure 6).

However, cellular GSH levels are subject to intracellular fluctuations [53]. Furthermore, GSH depletion typically occurs during oxidative stress and has been implicated in a variety of diseases, including Parkinson's disease, HIV and alcoholic liver disease [54]. Finally, also formaldehyde assimilation and ADH3-mediated oxidation to *S*-formylglutathione could result in very low local GSH concentrations. Such conditions might favour glutathione sulfinamide as the product, which is not metabolized further but is likely to yield glutathione sulfinic acid and perhaps also sulfonic acid, depending on the cellular redox state (Figure 6). These three compounds are associated with a gradual increase in inhibitory capacity for MGST1 (Figure 6, Table 5). The inhibition type was not assessed in the present study, but it has been shown for MGST1 that glutathione sulfonic acid exhibits competitive inhibition with respect to glutathione [22]. For evident structure similarity reasons, this is likely to also be the case for glutathione sulfinamide and sulfinic acid. Moreover, the results will probably be similar for other GSTs, considering that inhibition by glutathione sulfonic acid appears to be ubiquitous [22,55].

In conclusion, we have shown that ADH3-mediated GSNO reduction responds to ambient energy and redox state and is promoted by ADH3-dependent oxidative pathways *in vitro*. Our findings suggest two novel aspects of formaldehyde detoxification, both directly linked to the GSNOR activity of ADH3: first, formaldehyde could induce GSNO depletion and deregulate NO signalling pathways mediated through S-protein nitrosylation. Secondly, normal cellular GSH concentrations in the millimolar range prevent the conversion of GSNO into considerably strong inhibitors of GSTs, as demonstrated for MGST1. Still, under conditions of severe GSH depletion, the formation of glutathione sulfinamide and sulfinic acid might lead to a vicious cycle where cellular GSH-dependent defences are compromised and toxic responses exacerbated. However, the physiological relevance of glutathione sulfinamide and derived products relative to GSSG remains to be clarified. Overall, the results provide indirect evidence for formaldehyde as a physiological trigger of GSNO reduction and emphasize the importance of cellular redox state for GSNO metabolism.

© The Authors Journal compilation © 2008 Biochemical Society

We gratefully acknowledge Marie Ståhlberg and Åke Norberg for technical help and Masatoshi Nukui and Jaakko Patrakka for providing leftover mouse livers and lungs. We also thank Isaac Hashemy for valuable discussions on S-nitrosation and Professor Tomas Cronholm and Professor Jan Sjövall for critically reviewing this paper. Most parts of this work, which did not involve the use of preparations from laboratory animals, were supported by grants from the Swedish Cancer and Allergy Fund, the Swedish Fund for Research without Animal Experiments and the Swedish National Board of Laboratory Animals. Further funding was from the Swedish Cancer Society and Karolinska Institutet.

REFERENCES

1 Duester, G., Farres, J., Felder, M. R., Holmes, R. S., Höög, J. O., Parés, X., Plapp, B. V., Yin, S. J. and Jörnvall, H. (1999) Recommended nomenclature for the vertebrate alcohol dehydrogenase gene family. Biochem. Pharmacol. **58**, 389–395

2 Höög, J. O., Hedberg, J. J., Strömberg, P. and Svensson, S. (2001) Mammalian alcohol dehydrogenase — functional and structural implications. J. Biomed. Sci. **8**, 71–76

3 Hedberg, J. J., Höög, J. O., Nilsson, J. A., Xi, Z., Elfwing, Å. and Grafström, R. C. (2000) Expression of alcohol dehydrogenase 3 in tissue and cultured cells from human oral mucosa. Am. J. Pathol. **157**, 1745–1755

4 Hedberg, J. J., Griffiths, W. J., Nilsson, S. J. and Höög, J. O. (2003) Reduction of *S*-nitrosoglutathione by human alcohol dehydrogenase 3 is an irreversible reaction as analysed by electrospray mass spectrometry. Eur. J. Biochem. **270**, 1249–1256

5 Haqqani, A. S., Do, S. K. and Birnboim, H. C. (2003) The role of a formaldehyde dehydrogenase-glutathione pathway in protein S-nitrosation in mammalian cells. Nitric Oxide **9**, 172–181

6 Hess, D. T., Matsumoto, A., Kim, S. O., Marshall, H. E. and Stamler, J. S. (2005) Protein S-nitrosylation: purview and parameters. Nat. Rev. Mol. Cell Biol. **6**, 150–166

7 Khan, M., Sekhon, B., Giri, S., Jatana, M., Gilg, A. G., Ayasolla, K., Elango, C., Singh, A. K. and Singh, I. (2005) S-nitrosoglutathione reduces inflammation and protects brain against focal cerebral ischemia in a rat model of experimental stroke. J. Cereb. Blood Flow Metab. **25**, 177–192

8 Schonhoff, C. M., Matsuoka, M., Tummala, H., Johnson, M. A., Estevéz, A. G., Wu, R., Kamaid, A., Ricart, K. C., Hashimoto, Y., Gaston, B. et al. (2006) S-nitrosothiol depletion in amyotrophic lateral sclerosis. Proc. Natl. Acad. Sci. U.S.A. **103**, 2404–2409

9 Ju, T. C., Chen, S. D., Liu, C. C. and Yang, D. I. (2005) Protective effects of *S*-nitrosoglutathione against amyloid β-peptide neurotoxicity. Free Radical Biol. Med. **38**, 938–949

10 Que, L. G., Liu, L., Yan, Y., Whitehead, G. S., Gavett, S. H., Schwartz, D. A. and Stamler, J. S. (2005) Protection from experimental asthma by an endogenous bronchodilator. Science **308**, 1618–1621

11 Henderson, E. M. and Gaston, B. (2005) SNOR and wheeze: the asthma enzyme? Trends Mol. Med. **11**, 481–484

12 Wu, H., Romieu, I., Sienra-Monge, J. J., Estela Del Rio-Navarro, B., Anderson, D. M., Jenchura, C. A., Li, H., Ramirez-Aguilar, M., Del Carmen Lara-Sanchez, I. and London, S. J. (2007) Genetic variation in *S*-nitrosoglutathione reductase (GSNOR) and childhood asthma. J. Allergy Clin. Immunol. **120**, 322–328

13 Williamson, D. H., Lund, P. and Krebs, H. A. (1967) The redox state of free nicotinamide–adenine dinucleotide in the cytoplasm and mitochondria of rat liver. Biochem. J. **103**, 514–527

14 Zhang, Q., Piston, D. W. and Goodman, R. H. (2002) Regulation of corepressor function by nuclear NADH. Science **295**, 1895–1897

15 Grafström, R. C., Jernelöv, M.I., Dypbukt, J.M., Sundqvist, K., Atzori, L. and Zheng, X. (1996) Aldehyde toxicity and thiol redox state in cell cultures from human aerodigestive tract. In Correlations between *in Vitro* and *in Vivo* Investigations in Inhalation Toxicology (Saracci, R., ed.), pp. 319–336, ILSI Press, Washington DC

16 Lutz, W. K. (1990) Endogenous genotoxic agents and processes as a basis of spontaneous carcinogenesis. Mutat. Res. **238**, 287–295

17 Kucharczyk, N., Yang, J. T., Wong, K. K. and Sofia, R. D. (1984) The formaldehyde-donating activity of N^5,N^{10}-methylene tetrahydrofolic acid in xenobiotic biotransformation. Xenobiotica **14**, 667–676

18 Smith, T. J., Guo, Z., Gonzalez, F. J., Guengerich, F. P., Stoner, G. D. and Yang, C. S. (1992) Metabolism of 4-(methylnitrosamino)-1-(3-pyridyl)-1-butanone in human lung and liver microsomes and cytochromes P-450 expressed in hepatoma cells. Cancer Res. **52**, 1757–1763

19 Leikauf, G. D. (2002) Hazardous air pollutants and asthma. Environ. Health Perspect. **110**, (Suppl. 4), 505–526

20 Jensen, D. E., Belka, G. K. and Du Bois, G. C. (1998) S-nitrosoglutathione is a substrate for rat alcohol dehydrogenase class III isoenzyme. Biochem. J. **331**, 659–668

21 Liu, L., Hausladen, A., Zeng, M., Que, L., Heitman, J. and Stamler, J. S. (2001) A metabolic enzyme for S-nitrosothiol conserved from bacteria to humans. Nature **410**, 490–494

22 Sun, T. H. and Morgenstern, R. (1997) Binding of glutathione and an inhibitor to microsomal glutathione transferase. Biochem. J. **326**, 193–196

23 García-Sáez, I., Párraga, A., Phillips, M. F., Mantle, T. J. and Coll, M. (1994) Molecular structure at 1.8 Å of mouse liver class pi glutathione S-transferase complexed with *S*-(*p*-nitrobenzyl)glutathione and other inhibitors. J. Mol. Biol. **237**, 298–314

24 Hedberg, J. J., Strömberg, P. and Höög, J. O. (1998) An attempt to transform class characteristics within the alcohol dehydrogenase family. FEBS Lett. **436**, 67–70

25 Morgenstern, R. and DePierre, J. W. (1983) Microsomal glutathione transferase. Purification in unactivated form and further characterization of the activation process, substrate specificity and amino acid composition. Eur. J. Biochem. **134**, 591–597

26 Hart, T. W. (1985) Some observations concerning the S-nitroso and S-phenylsulphonyl derivatives of L-cysteine and glutathione. Tetrahedron Lett. **26**, 2013–2016

27 Sanghani, P. C., Stone, C. L., Ray, B. D., Pindel, E. V., Hurley, T. D. and Bosron, W. F. (2000) Kinetic mechanism of human glutathione-dependent formaldehyde dehydrogenase. Biochemistry **39**, 10720–10729

28 Arnelle, D. R. and Stamler, J. S. (1995) NO^+, NO, and NO-donation by S-nitrosothiols: implications for regulation of physiological functions by S-nitrosylation and acceleration of disulfide formation. Arch. Biochem. Biophys. **318**, 279–285

29 Takemoto, M., Asker, N., Gerhardt, H., Lundkvist, A., Johansson, B. R., Saito, Y. and Betsholtz, C. (2002) A new method for large scale isolation of kidney glomeruli from mice. Am. J. Pathol. **161**, 799–805

29a Bradford, M. M. (1976) A rapid and sensitive method for the quantitation of microgram quantities of protein utilizing the principle of protein–dye binding. Anal. Biochem. **72**, 248–254

30 Grafström, R. C. (2002) Human oral epithelium. In Culture of Epithelial Cells (Freshney, R. I. and Freshney, M.G ., eds), pp. 195–255, John Wiley and Sons, New York

31 Nilsson, J. A., Zheng, X., Sundqvist, K., Liu, Y., Atzori, L., Elfwing, Å., Arvidson, K. and Grafström, R. C. (1998) Toxicity of formaldehyde to human oral fibroblasts and epithelial cells: influences of culture conditions and role of thiol status. J. Dent. Res. **77**, 1896–1903

32 Singh, R. J., Hogg, N., Joseph, J. and Kalyanaraman, B. (1996) Mechanism of nitric oxide release from S-nitrosothiols. J. Biol. Chem. **271**, 18596–18603

33 Mani, A. R., Ebrahimkhani, M. R., Ippolito, S., Ollosson, R. and Moore, K. P. (2006) Metalloprotein-dependent decomposition of S-nitrosothiols: studies on the stabilization and measurement of S-nitrosothiols in tissues. Free Radical Biol. Med. **40**, 1654–1663

34 Sanghani, P. C., Davis, W. I., Zhai, L. and Robinson, H. (2006) Structure–function relationships in human glutathione-dependent formaldehyde dehydrogenase. Role of Glu-67 and Arg-368 in the catalytic mechanism. Biochemistry **45**, 4819–4830

35 Fernández, M. R., Biosca, J. A. and Parés, X. (2003) *S*-nitrosoglutathione reductase activity of human and yeast glutathione-dependent formaldehyde dehydrogenase and its nuclear and cytoplasmic localisation. Cell. Mol. Life Sci. **60**, 1013–1018

36 Lee, S. L., Wang, M. F., Lee, A. I. and Yin, S. J. (2003) The metabolic role of human ADH3 functioning as ethanol dehydrogenase. FEBS Lett. **544**, 143–147

37 Jourd'heuil, D., Laroux, F. S., Miles, A. M., Wink, D. A. and Grisham, M. B. (1999) Effect of superoxide dismutase on the stability of S-nitrosothiols. Arch. Biochem. Biophys. **361**, 323–330

38 Hou, Y., Guo, Z., Li, J. and Wang, P. G. (1996) Seleno compounds and glutathione peroxidase catalysed decomposition of S-nitrosothiols. Biochem. Biophys. Res. Commun. **228**, 88–93

39 Nikitovic, D. and Holmgren, A. (1996) *S*-nitrosoglutathione is cleaved by the thioredoxin system with liberation of glutathione and redox regulating nitric oxide. J. Biol. Chem. **271**, 19180–19185

40 Trujillo, M., Alvarez, M. N., Peluffo, G., Freeman, B. A. and Radi, R. (1998) Xanthine oxidase-mediated decomposition of S-nitrosothiols. J. Biol. Chem. **273**, 7828–7834

41 Cronholm, T. (1983) NAD^+-dependent ethanol oxidation: redox effects and rate limitation. Pharmacol. Biochem. Behav. **18**, (Suppl. 1), 229–232

42 Buchwalow, I. B., Minin, E. A., Samoilova, V. E., Boecker, W., Wellner, M., Schmitz, W., Neumann, J. and Punkt, K. (2005) Compartmentalization of NO signaling cascade in skeletal muscles. Biochem. Biophys. Res. Commun. **330**, 615–621

43 Iwakiri, Y., Satoh, A., Chatterjee, S., Toomre, D. K., Chalouni, C. M., Fulton, D., Groszmann, R. J., Shah, V. H. and Sessa, W. C. (2006) Nitric oxide synthase generates nitric oxide locally to regulate compartmentalized protein S-nitrosylation and protein trafficking. Proc. Natl. Acad. Sci. U.S.A. **103**, 19777–19782

44 Dales, R. and Raizenne, M. (2004) Residential exposure to volatile organic compounds and asthma. J. Asthma **41**, 259–270

45 Casset, A., Marchand, C., Purohit, A., le Calve, S., Uring-Lambert, B., Donnay, C., Meyer, P. and de Blay, F. (2006) Inhaled formaldehyde exposure: effect on bronchial response to mite allergen in sensitized asthma patients. Allergy **61**, 1344–1350

46 Gaston, B., Reilly, J., Drazen, J. M., Fackler, J., Ramdev, P., Arnelle, D., Mullins, M. E., Sugarbaker, D. J., Chee, C., Singel, D. J. et al. (1993) Endogenous nitrogen oxides and bronchodilator S-nitrosothiols in human airways. Proc. Natl. Acad. Sci. U.S.A. **90**, 10957–10961

© The Authors Journal compilation © 2008 Biochemical Society

47 Beltran, B., Orsi, A., Clementi, E. and Moncada, S. (2000) Oxidative stress and S-nitrosylation of proteins in cells. Br. J. Pharmacol. **129**, 953–960
48 Grafström, R. C. (1990) *In vitro* studies of aldehyde effects related to human respiratory carcinogenesis. Mutat. Res. **238**, 175–184
49 Deliconstantinos, G., Villiotou, V. and Stavrides, J. C. (1996) Increase of particulate nitric oxide synthase activity and peroxynitrite synthesis in UVB-irradiated keratinocyte membranes. Biochem. J. **320**, 997–1003
50 Kluge, I., Gutteck-Amsler, U., Zollinger, M. and Do, K. Q. (1997) *S*-nitrosoglutathione in rat cerebellum: identification and quantification by liquid chromatography-mass spectrometry. J. Neurochem. **69**, 2599–2607
51 Singh, S. P., Wishnok, J. S., Keshive, M., Deen, W. M. and Tannenbaum, S. R. (1996) The chemistry of the *S*-nitrosoglutathione/glutathione system. Proc. Natl. Acad. Sci. U.S.A. **93**, 14428–14433
52 Wong, P. S., Hyun, J., Fukuto, J. M., Shirota, F. N., DeMaster, E. G., Shoeman, D. W. and Nagasawa, H. T. (1998) Reaction between S-nitrosothiols and thiols: generation of nitroxyl (HNO) and subsequent chemistry. Biochemistry **37**, 5362–5371
53 Söderdahl, T., Enoksson, M., Lundberg, M., Holmgren, A., Ottersen, O. P., Orrenius, S., Bolcsfoldi, G. and Cotgreave, I. A. (2003) Visualization of the compartmentalization of glutathione and protein-glutathione mixed disulfides in cultured cells. FASEB J. **17**, 124–126
54 Townsend, D. M., Tew, K. D. and Tapiero, H. (2003) The importance of glutathione in human disease. Biomed. Pharmacother. **57**, 145–155
55 Dirr, H. W., Mann, K., Huber, R., Ladenstein, R. and Reinemer, P. (1991) Class pi glutathione S-transferase from pig lung. Purification, biochemical characterization, primary structure and crystallization. Eur. J. Biochem. **196**, 693–698

Received 12 December 2007/17 March 2008; accepted 16 April 2008
Published as BJ Immediate Publication 16 April 2008, doi:10.1042/BJ20071666

© The Authors Journal compilation © 2008 Biochemical Society